

The disease mutation A77V in Ryanodine receptor RyR2 induces changes in energy conduction pathways in the protein

B. Nazan Walpoth
Swiss Cardiovascular Center
University of Bern Inselspital
Cardiology, Bern Switzerland
NazanBeyhan.Walpoth@insel.ch

Burak Erman
Chemical and Biological Engineering, Koc University
Istanbul, Turkey
berman@ku.edu.tr

Abstract Energetically responsive residues of the 217 amino acid N-terminal domain of the cardiac Ryanodine receptor RyR2 are identified by a simple elastic net model. These residues lie along a hydrogen bonded path through the protein. The evolutionarily conserved residues of the protein are all located on this path or in its close proximity. All of the residues of the path are either located on the two Mir domains of the protein or are hydrogen bonded to them. Two calcium binding residues, E171 and E173, are proposed as potential binding residues, based on insights gained from the elastic net analysis of another calcium channel receptor, the inositol 1,4,5-triphosphate receptor, IP3R. Analysis of the disease causing A77V mutated RyR2 showed that the path is disrupted by the loss of energy responsiveness of certain residues.

The cardiac Ryanodine receptor has become a subject of increasing interest as its role in the etiology of cardiac disease became more apparent. Two genetic diseases have been linked to mutations in the cardiac Ryanodine receptor: arrhythmogenic right ventricular dysplasia type 2 (ARVD/C Typ 2 or simply ARVD/C) and catecholaminergic polymorphic ventricular tachycardia (CPVT) or familial polymorphic ventricular tachycardia. ARVD/C is an autosomal dominant cardiomyopathy, characterized by partial degeneration of the myocardium of the right ventricle, electrical instability, and sudden death. ARVD/C and CPVT can be caused by mutations in the cardiac Ryanodine receptor 2 gene (RyR2), located on chromosome 1q42.1–q43. There is a familial occurrence in about 50%. ARVD/C is characterized by fibrofatty replacement, primarily of the right ventricle¹. The gold standard for ARVD/C diagnosis is the demonstration of this alteration of ventricular myocardium, either postmortem or at surgery [2]. In the past 10 years, the identification of causative mutations in plakoglobin, desmoplakin, plakophilin-2, desmoglein-2, and desmocollin-2 has fostered the view that ARVD/C is a disorder of the desmosome and provided insight into its pathogenesis²⁻⁵. Desmosomal impairment followed by mechanical and electric uncoupling of cardiomyocytes leads to cell death with fibrofatty replacement⁶. Two nondesmosomal genes have been associated with specific types of ARVD/C: patients with CPVT have mutations in the cardiac Ryanodine receptor gene⁷.

The prevalence of ARVD/C is unknown, it is thought to occur in six per 10,000 persons in certain populations. Some studies have suggested that it may be as common as 1/1,000, reaching up to 1/200 in carriers of mutations relevant to ARVD/C, accounting for up to 17% of all sudden cardiac deaths in the young⁸. After hypertrophic heart disease, it is the number one cause of sudden cardiac death in young persons, especially athletes. The initial diagnosis of ARVD/C is based on the criteria established in 1994⁷ and revised in 2010⁹ including pathogenic mutations as a diagnostic criteria. After the diagnosis is made in one person, all of his or her first-degree relatives should be screened.

Treatment focuses on controlling the arrhythmias and in managing any signs or symptoms of heart failure. Antiarrhythmic medications are the initial and most commonly used therapy in ARVD/C. No single drug has been shown to be completely effective in controlling the arrhythmias. The therapeutic options are limited like pharmacological agents (ACEI, anticoagulants, diuretics, and antiarrhythmic agents as sotalol, verapamil, betablockers, amiodarone, and flecainide), catheter ablation to eliminate drug resistant conduction pathways (critical to the perpetuation of arrhythmias), implantable defibrillators in refractory patients at risk for sudden death and surgery as the last option, consisting on ventriculotomy and disconnection of the RV free wall or cardiac transplantation if severe terminal heart failure^{1,6,10,11}.

Thus, although ARVD/C is a clinically well defined disease, the molecular events underlying the disease phenotype have not reached an equal level of maturity. The specific aim of this paper is to understand the molecular forces behind the disease, and state them within a general molecular perspective.

There are essentially three forms, RyR1, RyR2 and RyR3. RyR1 is the channel in the skeletal muscle, RyR2 is the type expressed in the heart muscle, and RyR3 is found predominantly in the brain¹². Ca^{++} release from the sarcoplasmic reticulum, SR, mediated by the cardiac Ryanodine receptor (RyR2) is a fundamental event in cardiac muscle contraction. These receptors, which mediate the release of calcium from the SR to the cytosol, form a group of four homotetramers, with a large cytoplasmic assembly and a transmembrane domain called the pore region¹³. The first 4000 residues form the cytoplasmic region. The remaining 1777 residues, mostly helical in structure, form the transmembrane domain. The three dimensional structure of the full assembly is not known with high precision so as to merit structure based ligand design calculations. Effective computational methods are needed to characterize the various compartments of the assembly as effective targets¹⁴. However, the crystal structure of the first 217 amino acids of the N-terminal domain of the wild type RyR2 and its mutated form are determined with high precision by Petegem and Lobo^{15,16} which are adopted in the present paper for calculations.

In the diseased system, calcium leakage is the most important factor that can generate delayed after depolarizations, which can lead to fatal arrhythmias. More than 300 point mutations have been identified in the Ryanodine receptor some of which are associated with the disorders observed clinically^{8,17-19}. The present paper deals with one of these disease-causing point mutations, the A77V mutation. However, before analyzing the structural consequences of the mutation, we carry out a detailed analysis of the structural features of RyR2. We use a simple elastic net model²⁰ which is described in some detail in the Supplementary section. This model is based on the identification of residues that are responsive to conformational energy fluctuations of the protein. The energy responsive residues lie on a pathway which is regarded as the energy conduction pathway in the protein along which information is transmitted through correlated conformational fluctuations. We show here that the evolutionarily conserved residues lie on this path, thus pointing to the possible relation between conserved and energetically responsive amino acids. Identification of an energy conduction path in the protein establishes a reference structure. We show that the A77V mutation disrupts this pathway, thereby obliterating means of transferring information through the protein.

The N-terminal domain of RyR2 is a signal protein of 217 amino acids. The crystal structure of the N-terminal domain of physiological RyR2 (PDB code 3IM5) and the A77V mutated crystal structure (PDB code 3IM7) have been determined by x-ray with resolutions of 2.5 and 2.2 Å, respectively, by Van Petegem and Lobo¹⁵. The protein consists of a β -trefoil of 12 β strands held together by hydrophobic forces. A 10-residue α helix is packed against strands β 4 and β 5. A 3 residue 3-10 helix is present in the loop containing β 3 and β 4. The N-terminal contains two Mir domains, similar to inositol 1,4,5-triphosphate receptor (IP3R), for which ligand-induced conformational changes have been studied more extensively^{21,22}.

Results We report results of calculations based on the Elastic net Model of proteins explained briefly in the Methods section and in more detail in the Supplementary part.

The energy conduction path of RyR2: The residues that yield high values of the energy response are shown in Fig. 1, where the mean energy response ΔU_i of residue i is presented along the ordinate as a function of residue index. The circles indicate the conserved residues of 3IM5, obtained from the work of Ashkenazi et al²³ (See also the PDBSum web site²⁴). Comparison of the solid curve peaks and the circles shows that there is a strong correlation between the energy conduction path residues and conserved residues, in agreement with the recent suggestion of Lockless and Ranganathan²⁵. The set of

Figure-1

conserved residues, with highest level of conservation according to Reference 23 of the protein all lie within the set of energetically responsive residues and are located along or in the neighborhood of the energy conduction path. The peaks of Fig. 1 correspond to a path of spatially neighboring residues. These peaks correspond to pairs of neighboring residues that exhibit large energy fluctuation correlation values $\langle \Delta U_i \Delta U_j \rangle$ for the energy responsive residues i and j . In three dimensions, these residues are shown in Fig. 2a in yellow highlight. Fig. 2b is obtained by 90° rotation around the vertical axis. For a clearer representation, the path residues are shown and identified in Fig. 3. It is clearly seen that the path consists of residues that are hydrogen bonded to each other, as shown by the dashed lines.

Figure 2-a,b.

Figure-3

RyR2 contains two interspersed Mir domains, residues 124-178 and 164-217²⁶. Elastic net calculations show that the residues that lie on the energy conduction pathway are closely associated with the Mir domains. In Fig. 4, the secondary structures formed by all of the residues of Fig. 3 are shown. The secondary structures include portions of the Mir domains, such as the strands $\beta 8$ and $\beta 9$. Residues F145, C132, E171 and E173 are shown in ball and stick form. Five of the nine residues that are subject to disease causing mutations²⁷ either lie on the energy responsive path or are hydrogen bonded to the residues of the path. These are P164, R169, R176, V186, E189.

Figure-4.

The strands $\beta 8$ and $\beta 9$, which are parts of the Mir domain are central to this path as identified on the figure. Thus, the $\beta 8$ - $\beta 9$ loop is a hot spot for disease mutations, located at the inter-subunit interface²⁷. The path terminates with E171 and E173 at one end and with F145 at the other. E173 is also a disease mutation in RyR1 (E160G). The identification of the secondary structures as important components of energy transfer in proteins, which results from the application of the present elastic net model, have been suggested before²⁸, where such elements are found to increase the effectiveness of intramolecular communication. Mir domains of RyR2 plays an active role in energy transport through the protein. Below, we arrive at the same conclusion for the similar protein, the IP3R.

Effects of A77V mutation: The mutation A77V in RyR2 introduces two extra methyl groups, which induces rearrangements in the neighborhood of the mutation. However, these rearrangements appear to be correlated with the rest of the structure because there are large differences in the equilibrium

conformations of the two structures as may be verified from the difference map of Figure 5. The extent of conformational changes induced by the mutation may be understood by comparing the corresponding residue pair distances $R_{ij} = |\mathbf{R}_j - \mathbf{R}_i|$, where \mathbf{R}_i is the position vector of the i th C^α .

Figure-5

In Fig. 5, we plot the quantity $R_{ij} - R_{ij}^0$ for the two structures, wild type 3IM5 and A77V mutated 3IM7, as a function of residue pair indices ij , where the superscript zero denotes the wild type. The abscissa contains $n(n+1)/2 = 15051$ points corresponding to the residue pairs. Most of the distance differences are significant and above the uncertainties of the experimental resolution of 2.2-2.5 Å level. As will be shown below, the effects induced by these differences are not only local and confined to the vicinity of the mutation. The mutation introduces effects that are correlated with the overall protein structure, which in turn introduce modifications in the energy conduction pathway.

Elastic net calculations similar to the wild type are performed on the A77V mutated RyR2 in order to elucidate the differences between the energetically responsive residues. Results show that the energy conduction path observed in the wild type is disrupted in the mutated protein. The correlation data, $\langle \Delta U_i, \Delta U_j \rangle$, indicate that the residues shown in red in Fig. 6 are missing along the energy conduction path of the mutated protein. The identities of the missing residues are indicated in the figure.

Figure-6

Insights from the Inositol Receptor: The relationship between the structure and function of RyR2 is not well understood. IP3R, similar to RyR2 is a Ca^{2+} release channel, with structural similarity to RyR2. Both have a trefoil region each containing Mir domains. Two 3D structures of the receptor have been determined, with PDB codes of 1XZZ and 1N4K. 1N4K contains a calcium binding site with E283 and E285 that are similarly located in the RyR2 as E171 and E173, which emerge in our calculations as energetically important residues. Here, we apply the elastic net analysis to 1N4K. In Fig. 7, we present the energetically responsive residues (solid lines) and the conserved residues (circles) obtained by the elastic net analysis. Similar to RyR2, the conserved residues lie either on the energy conduction path or in its immediate neighborhood. In Fig. 8, we present the three dimensional picture of the protein, with the calculated energy correlation path shown in thick black lines. On the left of the figure, the green colored molecule is IP3. It makes one bond with R265 of the energy correlation path. On the right hand side, the two glutamic acid residues form the Calcium binding site. Similar to RyR2, the energetically responsive residues are located either on the Mir domain, or are hydrogen bonded to it.

Figure-7

Figure-8

Discussion: Using a simple computational model, we identified an energy conduction pathway for the wild type RyR2. This path whose residues are shown in Fig. 3 has several features of interest. Firstly, it contains most of the evolutionarily conserved residues. The remaining conserved residues are in the close neighborhood of the path, all making hydrogen bonds with the residues of the path. This important feature has recently been shown by Lockless and Ranganathan²⁵ implying that evolutionary conservation is driven by energy conduction in proteins. Although no ligands for RyR2 N-terminal have been observed until now²⁹, the two glutamic acids, E171 and E173 on the extremity of the path may potentially form a calcium binding site. This suggestion is based on the observation that in IP3R a potential calcium binding site is formed by E283 and E285 whose location on the path coincides

exactly with that of RyR2. That the residue E173 (E164 in RyR1) is exposed to water and is a candidate for possible binding. E171 and E173 (which correspond to human RyR1 residues 158 and 160; or rabbit RyR1 residues 159 and 161 in pdb 1XOA, are located near interfaces 1 and 4 as identified by Tung et al.²⁷. The correspondence of the glutamic acid sites for the two proteins, RyR2 and IP3R can be seen by comparing Figs. 3 and 8. Several residues of the energy conduction path of the wild type RyR2 disappear on the path of the disease causing A77V mutation. Among the disappearing residues is E171, as well as several others on the two extremities of the path as identified and shown in red in Fig. 6. The loss of energy response of these residues is expected to disrupt signal conduction that would otherwise result from the correlated fluctuations of the residues along the path. These suggestions are based on the elastic net analysis of the more widely studied calcium channel receptor IP3R. Five of the nine disease causing mutations of molecule A of RyR2 N-terminal are on the calculated energy conduction path. V186 sits at the apex of $\beta 8$ and $\beta 9$. $\beta 8$ is demarcated by V186 and P164. R176 and R169 are in the close spatial neighborhood of P164. These observations point to the close association between energy conduction path residues, evolutionarily conserved residues, the Mir domains, and disease causing residues.

Methods:

Determining the energy conduction path: Elastic net models are simple, C^α based coarse grained models which can identify residues that play important role on the energetic interactions of the protein. A detailed explanation of the model that identifies the residues taking part in energy transfer is given in the Supplementary section. Stated briefly, the picture is as follows: Fluctuations ΔR_i in the position of a residue i , resulting from thermal energy, cause the atoms of the residue to interact with the atoms of the neighboring residues. On the average, a residue has about twelve neighboring residues that it directly interacts with. These fluctuation based interactions induce changes in the energy of the residue and its neighbors because the distance between each interacting i th and j th residues changes. The resulting fluctuation of the energy over the distance R_{ij} is $\Delta \hat{U}_{ij}$. The hat over U denotes that this is an instantaneous value. The energetic interaction of residue i with all other residues of the protein is expressed by the sum $\Delta \hat{U}_i = \sum_j \Delta \hat{U}_{ij}$. The energy response $\Delta \hat{U}_i$ of i may be correlated with the energy response $\Delta \hat{U}_j$ of residue j . This correlation is given with the nonzero value of the average $\langle \Delta \hat{U}_i \Delta \hat{U}_j \rangle$ where the angular brackets denote an average over all instantaneous fluctuations. Summing up over the fluctuations of the j th residue leads to the energy response ΔU_i of residue i as $\Delta U_i = \sum_j \langle \Delta \hat{U}_i \Delta \hat{U}_j \rangle$. This is a thermodynamically meaningful quantity showing the mean energy response of residue i to all fluctuations of its surroundings. These correlations extend throughout the protein, leading to specific paths along which the fluctuations propagate. Recent work shows that these paths are evolutionarily conserved²⁵. The simplest elastic net model assumes harmonic fluctuations of the residues and the energies²⁰. More sophisticated versions of elastic networks introduce anharmonicities into the model for more accurate results at the expense of simplicity. We apply the harmonic model to the analysis of wild type RyR2 and its A77V mutated form.

Acknowledgment: We are grateful for the suggestions of Professor Filip van Petegem for insightful suggestions which have been incorporated into the final version of the manuscript.

References

1. Patel, H.C. & Calkins, H. Arrhythmogenic right ventricular dysplasia. *Current treatment options in cardiovascular medicine*, 598-613 (2010).

2. Gerull, B. et al. Mutations in the desmosomal protein plakophilin-2 are common in arrhythmogenic right ventricular cardiomyopathy (vol 36, pg 1162, 2004). *Nature Genetics* **37**, 106-106 (2005).
3. Pilichou, K. et al. Mutations in desmoglein-2 gene are associated to arrhythmogenic right ventricular cardiomyopathy. *European Heart Journal* **27**, 294-294 (2006).
4. McKenna, W.J., Sen-Chowdhry, S. & Syrris, P. Genetics of right ventricular cardiomyopathy. *Journal of Cardiovascular Electrophysiology* **16**, 927-935 (2005).
5. McKenna, W.J. et al. Arrhythmogenic right ventricular dysplasia/cardiomyopathy associated with mutations in the desmosomal gene desmocollin-2. *American Journal of Human Genetics* **79**, 978-984 (2006).
6. Saffitz, J.E. et al. Structural and molecular pathology of the heart in Carvajal syndrome. *Cardiovascular Pathology* **13**, 26-32 (2004).
7. Abraham, T.P. et al. Comparison of novel echocardiographic parameters of right ventricular function with ejection fraction by cardiac magnetic resonance. *Journal of the American Society of Echocardiography* **20**, 1058-1064 (2007).
8. Marks, A.R. & Betzenhauser, M.J. Ryanodine receptor channelopathies. *Pflugers Archiv-European Journal of Physiology* **460**, 467-480 (2010).
9. Cox, M.G.P.J. et al. Arrhythmogenic Right Ventricular Dysplasia/Cardiomyopathy Diagnostic Task Force Criteria Impact of New Task Force Criteria. *Circulation-Arrhythmia and Electrophysiology* **3**, 126-133 (2010).
10. Moric-Janiszewska, E. & Markiewicz-Loskot, G. Review on the genetics of arrhythmogenic right ventricular dysplasia. *Europace* **9**, 259-266 (2007).
11. Danieli, G.A. et al. Identification of mutations in the cardiac ryanodine receptor gene in families affected with arrhythmogenic right ventricular cardiomyopathy type 2 (ARVD2). *Human Molecular Genetics* **10**, 189-194 (2001).
12. Kimlicka, L. & Van Petegem, F. The structural biology of ryanodine receptors. *Science China-Life Sciences* **54**, 712-724 (2011).
13. <http://www.uniprot.org/uniprot/Q92736>.
14. Hamilton, S.L. & Serysheva, I.I. Ryanodine Receptor Structure: Progress and Challenges. *Journal of Biological Chemistry* **284**, 4047-4051 (2009).
15. Van Petegem, F. & Lobo, P.A. Crystal Structures of the N-Terminal Domains of Cardiac and Skeletal Muscle Ryanodine Receptors: Insights into Disease Mutations. *Structure* **17**, 1505-1514 (2009).
16. Van Petegem, F., Lobo, P.A., Kimlicka, L. & Tung, C.C. The Deletion of Exon 3 in the Cardiac Ryanodine Receptor Is Rescued by beta Strand Switching. *Structure* **19**, 790-798 (2011).
17. Van Petegem, F. & Kimlicka, L. The structural biology of ryanodine receptors. *Science China-Life Sciences* **54**, 712-724 (2011).
18. Priori, S.G. & Chen, S.R.W. Inherited Dysfunction of Sarcoplasmic Reticulum Ca(2+) Handling and Arrhythmogenesis. *Circulation Research* **108**, 871-883 (2011).
19. Williams, A.J., Thomas, N.L., Maxwell, C. & Mukherjee, S. Ryanodine receptor mutations in arrhythmia: The continuing mystery of channel dysfunction. *Febs Letters* **584**, 2153-2160 (2010).
20. Erman, B. Relationships between ligand binding sites, protein architecture and correlated paths of energy and conformational fluctuations. *Physical Biology* **8**, 056003 (9pp) (2011).
21. Lin, C.C., Baek, K. & Lu, Z. Apo and InsP(3)-bound crystal structures of the ligand-binding domain of an InsP(3) receptor. *Nature Structural & Molecular Biology* **18**, 1172-1174 (2011).
22. Yuchi, Z.G. & Van Petegem, F. Common allosteric mechanisms between ryanodine and inositol-1,4,5-trisphosphate receptors. *Channels* **5**, 120-123 (2011).
23. Ashkenazi, H., Erez E., Martz, E., Pupko, T. & N., B.-T. ConSurf 2010: calculating evolutionary conservation in sequence and structure of proteins and nucleic acids. *Nucleic Acids Research* **38**, W529-W533 (2010).
24. PDBSUM. <http://www.ebi.ac.uk/pdbsum/>.
25. Lockless, S.W. & Ranganathan, R. Evolutionarily conserved pathways of energetic connectivity in protein families. *Science* **286**, 295-299 (1999).

26. Amador, F.J. et al. Crystal structure of type 1 ryanodine receptor amino-terminal beta-trefoil domain reveals a disease-associated mutation "hot spot" loop. *Proceedings of the National Academy of Sciences of the United States of America* **106**, 11040-11044 (2009).
27. Tung, C.C., Lobo, P.A., Kimlicka, L. & Van Petegem, F. The amino-terminal disease hotspot of ryanodine receptors forms a cytoplasmic vestibule. *Nature* **468**, 585-U267 (2010).
28. Chennubhotla, C. & Bahar, I. Signal propagation in proteins and relation to equilibrium fluctuations. *Plos Computational Biology* **3**, 1716-1726 (2007).
29. van Petegem, F. Private correspondence .

Figure captions

Figure 1. Energetically responsive residues (solid line) obtained with the elastic net model (See Supplementary section), and the conserved residues (circles) obtained from Reference 24. In Reference 23, conservation levels are ordered from 1 to 8, the latter denoting the highest degree of conservation. The filled circles correspond to residues with level 8. The ordinate values are in arbitrary un-normalized units.

Figure 2a. Residues, highlighted in yellow, along the energy conduction path in RyR2. Figure 2b. 90° rotated depiction of Figure 2a.

Figure 3. Residues along the energy conduction pathway. Green dashed lines denote the hydrogen bonds.

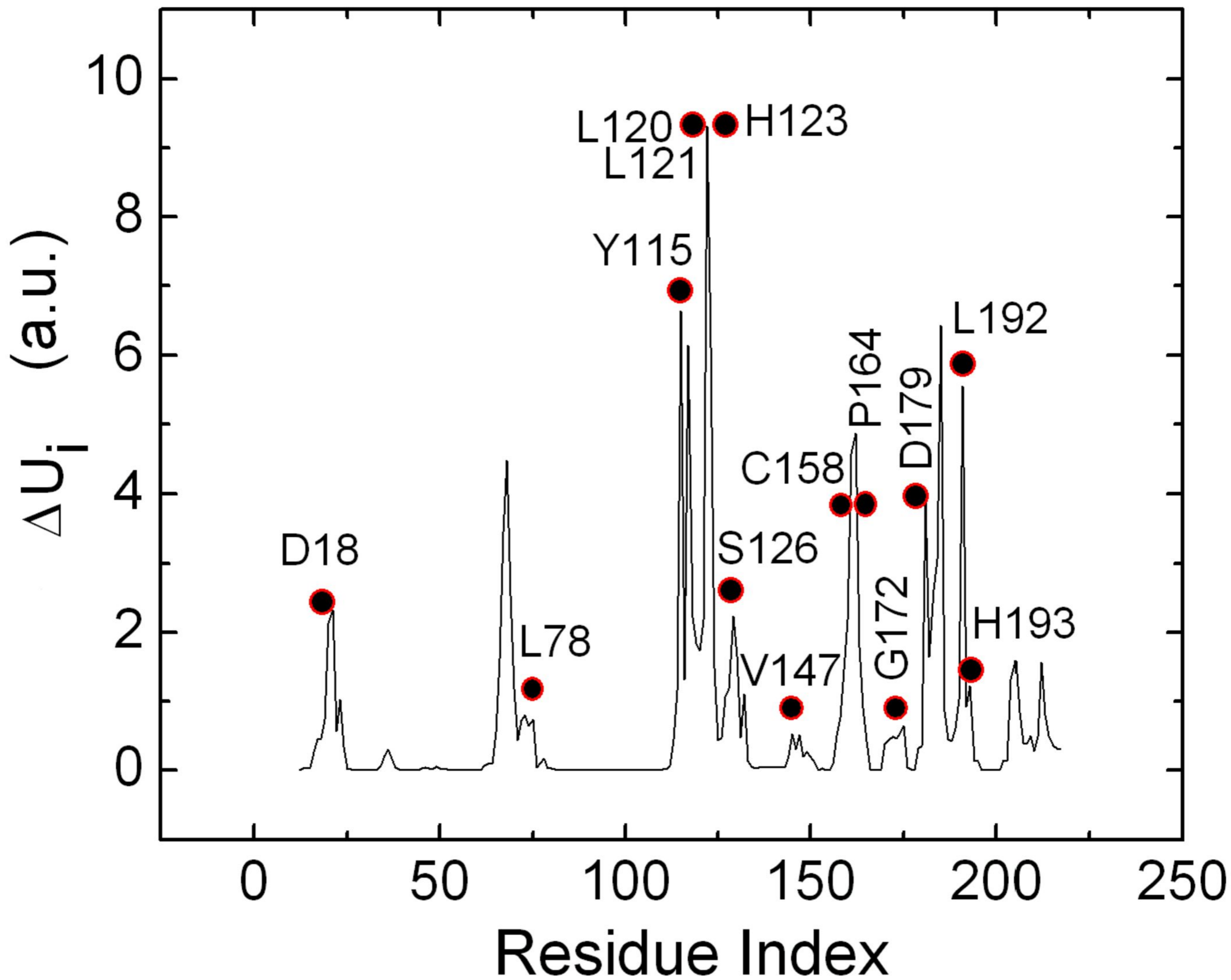
Figure 4. The energy responsive path showing the residues (in green) that exhibit disease causing mutations²⁷. The strands $\beta 8$ and $\beta 9$, which are parts of the Mir domain are also identified.

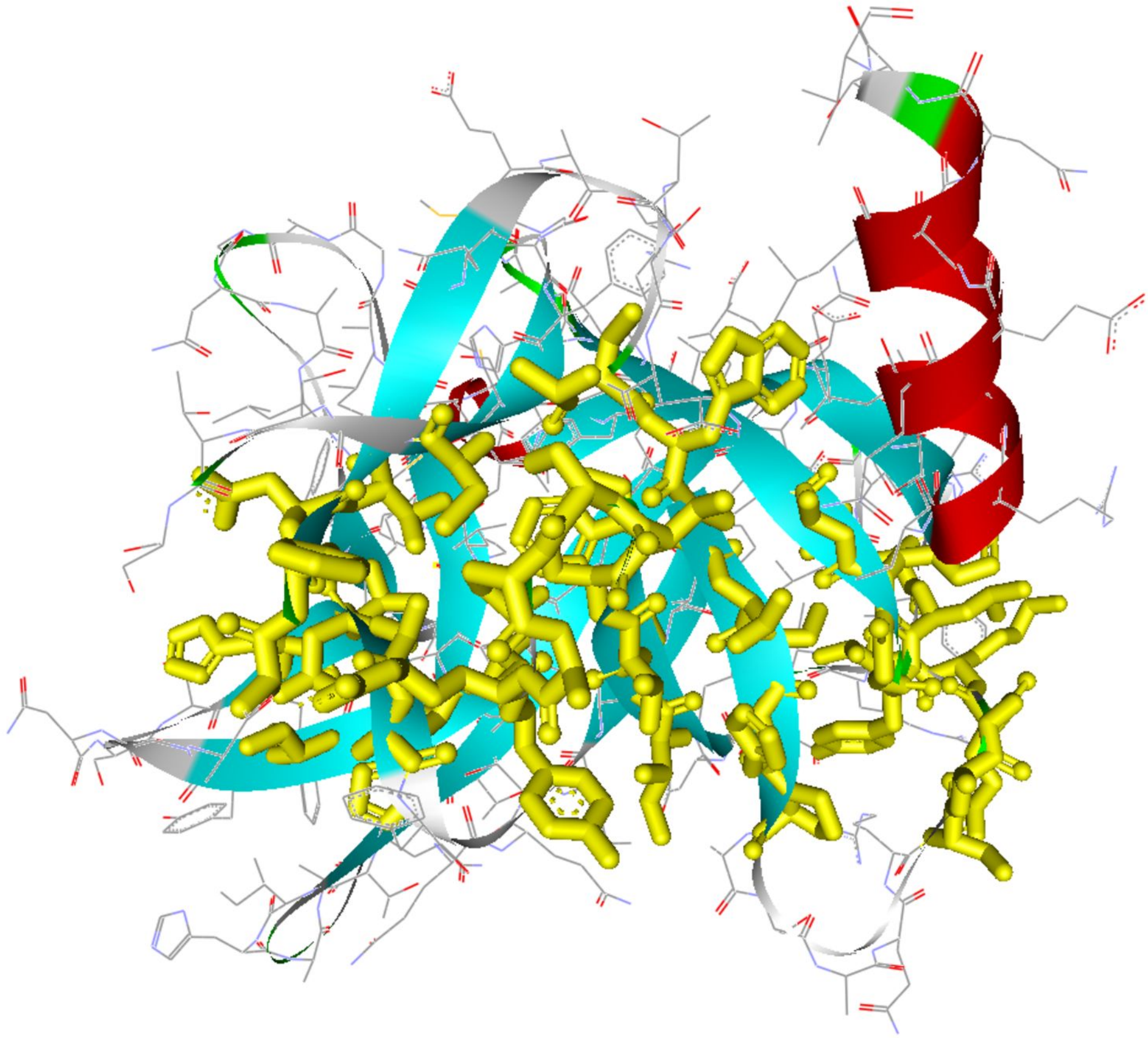
Figure 5. The differences between $R_{ij} - R_{ij}^0$ of the mutated and wild type C^α separations.

Figure 6. The residues that loose correlation upon mutation, shown in red and identified by residue type and number.

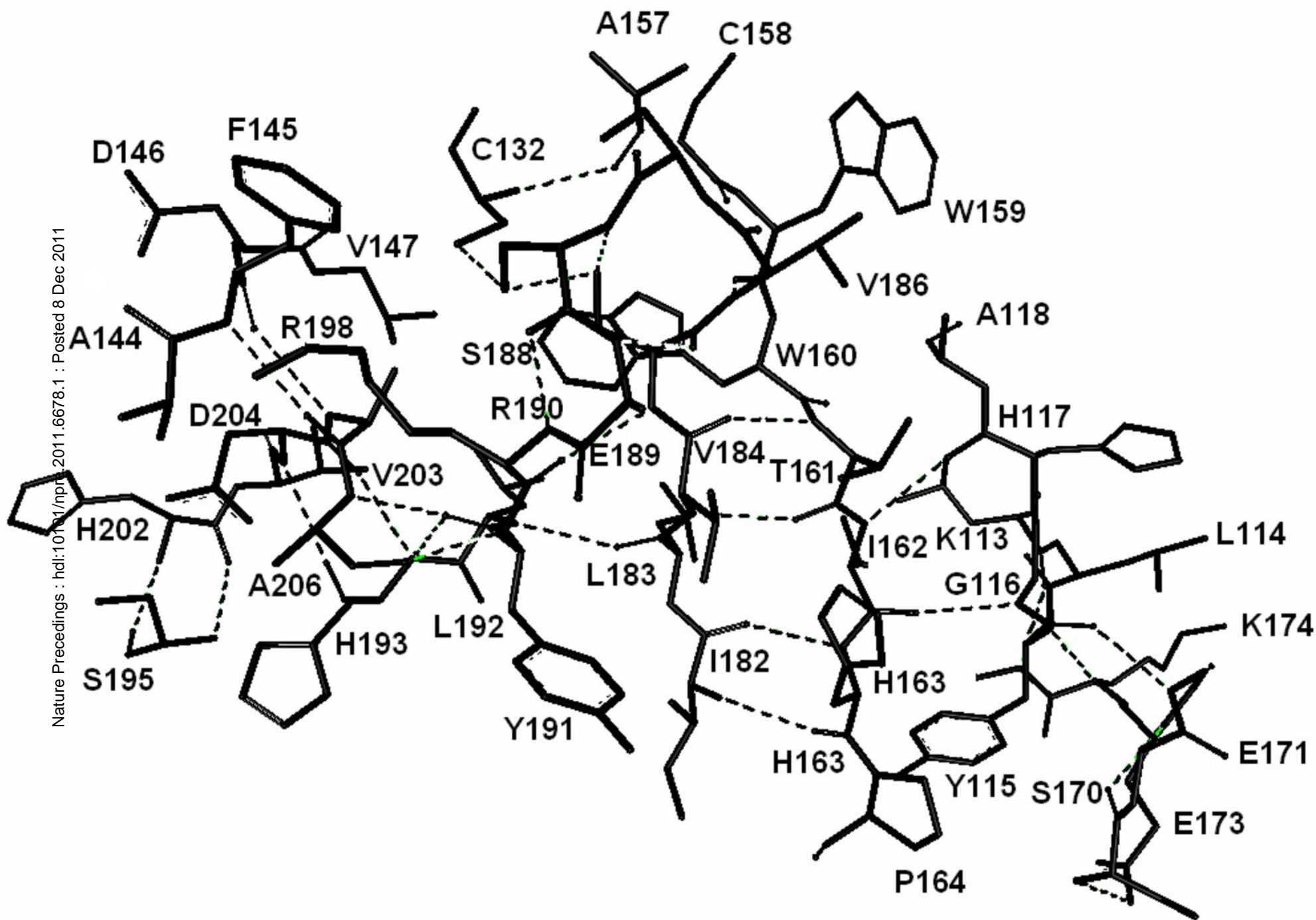
Figure 7. Energetically responsive residues (solid line) and the conserved residues (circles) of the trefoil part of 1N4K. See the legend for Fig. 1.

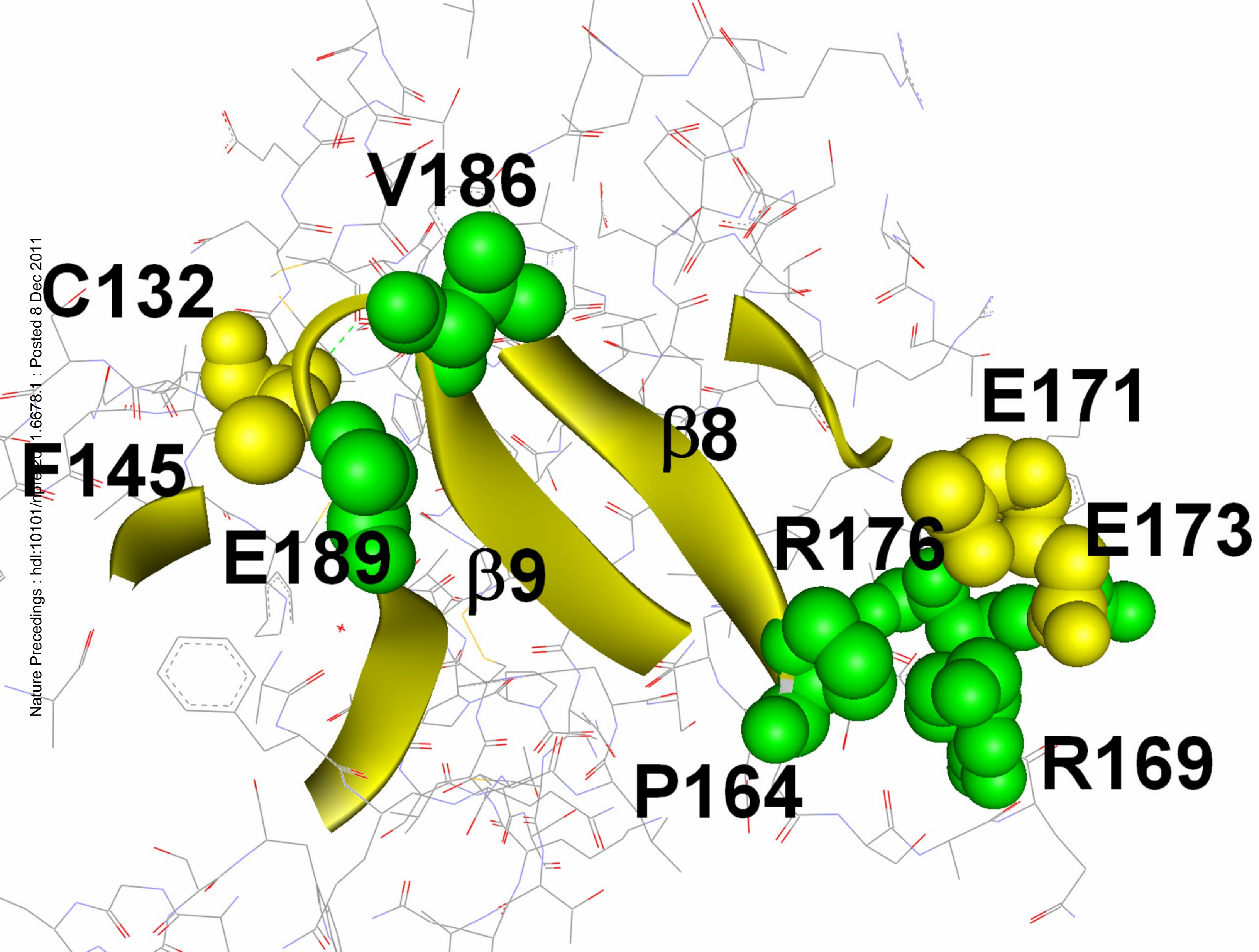
Figure 8. Energetically responsive residues of IP3R highlighted in black. The green colored molecule is IP3. On the right of the path, the two residues E283 and E285 constitute the potential calcium binding site. The offset shows the binding mode of calcium to the two residues, the green dashed lines are the hydrogen bonds.











V186

C132

E145

E189

$\beta 9$

P164

$\beta 8$

R176

R169

E171

E173

